Global Change Biology

Global Change Biology (2010) **16**, 1762–1776, doi: 10.1111/j.1365-2486.2009.02032.x

On the relationship between water table depth and water vapor and carbon dioxide fluxes in a minerotrophic fen

O. SONNENTAG*, G. VAN DER KAMP†, A. G. BARR‡ and J. M. CHEN§

*University of California Berkeley, Department of Environmental Science, Policy and Management, 121 Mulford Hall, Berkeley, CA 94720, USA, †National Water Research Institute, Environment Canada, 11 Innovation Boulevard, Saskatoon, SK, Canada S7N 3H5, ‡Climate Research Division, Environment Canada, 11 Innovation Boulevard, Saskatoon, SK, Canada S7N 3H5, §University of Toronto, Department of Geography and Program in Planning, St George Campus, Sidney Smith Hall, 100 St George St., Room 5047, Toronto, ON, Canada M5S 3G3

Abstract

The focus of this study is the relationship between water table depth (WTD) and water vapor [evapotranspiration (ET)] and carbon dioxide [CO_2; net ecosystem exchange (NEE)] fluxes in a fen in western Canada. We analyzed hydrological and eddy covariance measurements from four snow-free periods (2003–2006) with contrasting meteorological conditions to establish the link between daily WTD and ET and gross ecosystem CO_2 exchange (GEE) and ecosystem respiration (R_{eco}; NEE = R_{eco}−GEE), respectively: 2003 was warm and dry, 2004 was cool and wet, and 2005 and 2006 were both wet. In 2003, the water table (WT) was below the ground surface. In 2004, the WT rose above the ground surface, and in 2005 and 2006, the WT stayed well above the ground surface. There were no significant differences in total ET ($\sim$ 316 mm period^{-1}), but total NEE was significantly different (2003: 8 g C m^{-2} period^{-1}; 2004: −139 g C m^{-2} period^{-1}; 2005: −163 g C m^{-2} period^{-1}; 2006: −195 g C m^{-2} period^{-1}), mostly due to differences in total GEE (2003: 327 g C m^{-2} period^{-1}; 2004: 513 g C m^{-2} period^{-1}; 2005: 411 g C m^{-2} period^{-1}; 2006: 556 g C m^{-2} period^{-1}). Variation in ET is mostly explained by radiation (67%), and the contribution of WTD is only minor (33%). WTD controls the compensating contributions of different land surface components, resulting in similar total ET regardless of the hydrological conditions. WTD and temperature each contribute about half to the explained variation in GEE up to a threshold ponding depth, below which temperature alone is the key explanatory variable. WTD is only of minor importance for the variation in R_{eco}, which is mainly controlled by temperature. Our study implies that future peatland modeling efforts explicitly consider topographic and hydrogeological influences on WTD.

Keywords: evapotranspiration, net ecosystem CO_2 exchange, Northern Peatlands, water table depth, water use efficiency

Received 9 March 2009 and accepted 7 July 2009

Introduction

Northern (i.e. boreal and subarctic) peatlands encompass a diverse range of water-logged ecosystems that accumulate carbon (C) in the form of peat due to the slight but persistent exceedance of net primary productivity (NPP) over the decomposition of organic matter. Northern peatlands in Eurasia and North America have accumulated C at a mean long-term rate of 15–30 g C m^{-2} yr^{-1} since their formation 6000–10000 years ago, after the last deglaciation (e.g., Gorham, 1991; Turunen *et al*., 2002). As a result, northern peatlands now store up to one-third of the global soil C, while covering only about 3% of the terrestrial land surface (Gorham, 1991; Maltby & Immirzi, 1993). Northern peatlands are important in the global C cycle from a climate change perspective because they act as long-term sinks of carbon dioxide (CO_2) and sources for methane (CH_4) and export dissolved organic carbon (DOC) (Moore *et al*., 1998). Water table depth (WTD) and peat volumetric soil moisture content constitute primary controls over northern peatlands' long-term CO_2 sink and CH_4 source strengths since they determine the zones of aerobic and anaerobic conditions. Complete multi-year annual peatland C balances

Correspondence: O. Sonnentag, tel. + 1 510 642 8322, fax + 1 510 642 1477, e-mail: oliver.sonnentag@berkeley.edu

(e.g., Roulet *et al.*, 2007; Nilsson *et al.*, 2008) for years of contrasting meteorological conditions are still rare. Thus, the response of northern peatlands' hydrological and C cycle processes to changing climate is complex, and the fate of northern peatlands' CO_2 sink and CH_4 source remains uncertain.

A commonly used classification for northern peatlands is based on their water balance and resulting nutrient status and distinguishes between bogs and fens. Bogs are fed by precipitation only (ombrotrophic) and other hydrological inputs are considered negligible. Fens, commonly subdivided into rich and poor fens, are alkaline and nutrient-rich peatlands due to additional hydrological inputs in the form of surface and subsurface flow (minerotrophic).

An important component of the peatland water balance is precipitation minus evapotranspiration (P−ET) (Roulet *et al.*, 1997), i.e. the net atmospheric flux of water, where ET represents the latent heat (λE) flux of the peatland surface energy balance. ET is dependent on meteorological and environmental conditions, and in turn has the potential to control peatland C dynamics through the peatland water balance.

A series of studies have shed light on the relative importance of hydrological and environmental controls on water vapor and CO_2 fluxes in northern peatlands using techniques such as chamber and eddy covariance (EC) flux measurements and process-oriented ecosystem modeling (e.g., Bubier *et al.*, 2003; Yurova *et al.*, 2007; Sagerfors *et al.*, 2008). Some studies identified WTD as the major control on net ecosystem CO_2 exchange (NEE) or its component fluxes of photosynthesis [gross ecosystem exchange (GEE)] and total ecosystem respiration (R_{eco}) (e.g., Arneth *et al.*, 2002). Other studies concluded that WTD was a less important control than light, and air (T_{air}) or soil temperature (T_{soil}) (e.g. Lafleur *et al.*, 2005b). Similarly, contrasting evidence on the influence of WTD on peatland ET is provided in the literature (e.g., Lafleur *et al.*, 2005a; Humphreys *et al.*, 2006). In a review, Roulet *et al.* (1997) concluded that ET from bogs and poor fens is generally lower than from other peatland types as a result of the complex interaction between WTD and factors such as topography, vegetation composition, and meteorological conditions. These studies provide important insights into the role of various controls on peatland functioning for a range of peatland types in different climatic settings.

Here, we report 4 years of EC and supporting measurements (May 1–October 31, 2003–2006) for the Sandhill fen in central Sasketchawan, Canada. The goal is to explore the relationship between daily fluctuations in WTD and water vapor and CO_2 fluxes. To meet this goal, we first assess changes in WTD in response to dry and wet meteorological conditions. Next we compare diurnal and daily variations in ET and NEE and its component fluxes GEE and R_{eco}, and assess the relative importance of WTD, radiation (ET) and temperature (GEE, R_{eco}) as controlling factors.

Materials and methods

Site description

The Sandhill fen (SF; 53.80°N, 104.62°W) site is located within the Boreal Plain ecoregion of western Canada, about 115 km northeast of Prince Albert, Saskatchewan. The Northwest-Southeast-oriented 8.5 km^2 peatland is classified as open, minerotrophic, and moderately rich fen (Zoltai *et al.*, 2000). It was the fen site of the southern study area (SSA; Suyker *et al.*, 1997) of the Boreal Ecosystem Atmosphere Study (BOREAS; Sellers *et al.*, 1997) and is now one of the peatland sites of the Canadian Carbon Program (CCP; http://www.fluxnet-canada.ca). The climate of the area is classified as subhumid with a mean annual total P of 467 mm [Environment Canada 1971–2000 climate normals) for Waskesiu Lake (53.92°N, 106.07°W)]. The mean annual T_{air} is 0.4 °C, with mean monthly T_{air} ranging from −17.9 °C (January) to 16.2 °C (July). The winter season usually begins in early November and lasts until April.

The SF site is situated in an open depression within Pleistocene glacial deposits. The 'drier' margins of the SF site are elevated (<1 m) and inclined toward its center. The ground surface pattern in the open and generally 'wetter' central portion (~ 2.4 km^2) is caused by East–West-oriented ridges and adjoining swales, i.e. topographic depressions, with a relief of about 0.25–0.30 m. The swales are interspersed with hummocks and hollows with a relief of about 0.20 m. Ground surface elevation changes follow changes in WTD within 0.20 m (Hogan, 2005). The elevated margins are dominated by shallow peat with a depth between 0.5 and 1.0 m. Peat depth increases to ~ 3.3 m in the open, central portion of the SF site. Lateral saturated hydraulic conductivity was determined to be as high as $9 \times 10^{-3}\,m\,s^{-1}$ for the less decomposed peat at the ground surface, and as low as 10^{-6} to $10^{-5}\,m\,s^{-1}$ at depths of >2 m (Hogan *et al.*, 2006).

The multi-scale topographic features are well-reflected in wetness and vegetation composition, comprising <10 m-high tamarack (*Larix laricina*) trees over <0.5 m-high evergreen (bog rosemary; *Andromeda polifolia*) and deciduous (dwarf birch; *Betula glandulosa*) shrubs and various species of dominating sedges (e.g., mostly *Carex spp.*, *Eriphorum spp.*) over a discontinuous ground cover dominated by brown mosses on drier ridges. Wetter swales are mostly covered by ~ 0.2 m-high sedges, dwarf birch, and herbs such as buck bean

(*Menyanthes tridoliata*), and <2 m-high tamarack trees (missing in the open portion of the SF site) in wetter swales. Mean tree leaf area index (LAI) [standard deviation (SD)] along a 200-m transect was estimated in October 2003, a relatively dry year when the WT was well below the ground surface (Meteorological and resulting hydrological conditions). Tree LAI increased from 0.38 (0.08) at the center of the SF site to 1.29 (0.06) near the margins (Bhatti *et al*., 2006). Similar values for tree LAI were obtained in August 2006 (unpublished data), which was a relatively wet year. Shrub/sedge LAI measured along several 200-m transects in August 2006 (unpublished data) when the WT was above the ground surface had a mean value (SD) of 1.57 (0.79). Unfortunately, shrub/sedge LAI was not measured in 2003 and aboveground biomass measurements do not exist. However, we observed that under dry conditions the abundance of green shrubs increased while the abundance of dominating sedges was substantially lower due to earlier senescence. This observation is in accordance with other studies in fens dominated by *Carex* spp. reporting stressed vegetation in drier compared with wetter years (e.g., Griffis *et al*., 2000; Bubier *et al*., 2003).

EC and supporting measurements

Sensible (H; $\mathrm{W\,m^{-2}}$) and latent heat (λE; $\mathrm{W\,m^{-2}}$), and CO_2 (F_c; $\mu\mathrm{mol\,m^{-2}\,s^{-1}}$) flux densities between the SF site and the atmosphere, and the change in CO_2 storage (F_s; $\mu\mathrm{mol\,m^{-2}\,s^{-1}}$) between the ground surface and the instrumentation height were measured by the EC technique. A 15-m scaffold micrometeorological tower was located about 150 m west of the eastern margin in the open, southern half of the SF site. The EC instrumentation was mounted on the tower on a 4-m boom oriented toward the West (prevailing wind direction) at a height of 3 m above the mean ground surface. The EC instrumentation comprised an open-path infrared gas analyzer (IRGA; model LI-7500; LI-COR, Lincoln, NE, USA) to measure the molar densities of CO_2 (ρ_{CO_2}; $\mathrm{mmol\,m^{-3}}$) and water vapor (ρ_{H_2O}; $\mathrm{mmol\,m^{-3}}$), a three-dimensional sonic anemometer-thermometer (3D-SAT; model CSAT3, Campbell Scientific, Logan, UT, USA) to measure zonal, meridional, and vertical wind velocities (u; v; w; $\mathrm{m\,s^{-1}}$) and sonic air temperature (T_{sonic}; °C), and a fine-wire thermocouple (25 μm in diameter) to measure air temperature ($T_{air\text{-}fine}$; °C). The high-frequency digital signals from these three instruments were recorded by a personal computer at a scan rate of 20 Hz. The upwind fetch of the tower was roughly estimated as 300 m to the West and as 600–800 m to Southwest and Northwest, respectively (Suyker *et al*., 1997).

Supporting meteorological and environmental measurements were made at the tower or in close proximity. These included incoming and outgoing shortwave (K_{in}; K_{out}; $\mathrm{W\,m^{-2}}$), longwave (L_{in}; L_{out}; $\mathrm{W\,m^{-2}}$) and net (R_{net}; $\mathrm{W\,m^{-2}}$) radiation measured using a four-component net radiometer (model CNR1, Kipp and Zonen, Delft, the Netherlands). The radiometer was mounted on a 4-m boom at a height of 15 m and oriented to the South. Incoming and outgoing photosynthetically active radiation (PAR_{in}; PAR_{out}; $\mu\mathrm{mol\,m^{-2}\,s^{-1}}$) were measured with quantum sensors (model LI190sa; LI-COR). Relative humidity ($U_{2\,m}$; %) and air temperature ($T_{air\_2\,m}$; °C) were both measured at 2 m above the average ground surface (model HMP45CF; Campbell Scientific). Precipitation (P; mm) was measured with an accumulating gauge (model Belfort 750 with an Alter shield; Belfort, Baltimore, MD, USA) at a height of 2 m. Both wind speed (u; $\mathrm{m\,s^{-1}}$) and direction were measured at a height of 15 m using a propeller anemometer and vane (model 05103; R. M. Young, Traverse City, MI, USA). Soil temperature (T_{soil}; °C) was measured using chromel-constantan thermocouples at eight depths (0, 0.05, 0.1, 0.2, 0.3, 0.5, 0.75, 1.0, and 1.25 m) below the ground surface about 50 m east of the tower and in a drier ridge ($T_{soil\text{-}ridge}$) and an adjacent wetter swale ($T_{soil\text{-}swale}$), about 200 m west of the tower. At the ridge and swale, ponded-water temperature (T_{water}; °C) was measured using chromel-constantan thermocouples at 0.05 m above the ground surface. Ground heat flux (G; $\mathrm{W\,m^{-2}}$) was measured in two ways: using four heat flux plates (model HFP01; Hukseflux Thermal Sensors, Delft, the Netherlands) buried at a depth of 0.1 m (corrected for heat storage above the plates), and based on heat storage changes in the peat and ponded water, integrated to 1.25 m depth, estimated when the WT was approximately at the ground surface. Because the ponded-water temperature was measured at 5-cm height only, it was not possible to calculate G when the ponded water was deeper, excluding many periods in 2004–2006. All meteorological variables were logged by a datalogger (model CR23x, Campbell Scientific) using a scan period of 5 s and recorded as half-hourly mean values.

Data handling and processing of EC measurements

Half-hourly mean fluxes of H, λE and F_c were calculated from the high-frequency data of $T_{air\text{-}fine}$, T_{sonic}, u, v, w, ρ_{H_2O}, and ρ_{CO_2} measured with the EC instrumentation. To remove the effect of air density fluctuations, ρ_{H_2O} and ρ_{CO_2} were converted to H_2O and CO_2 mole-mixing ratios, S_{CO_2} and S_{H_2O}, respectively (Webb *et al*., 1980). Furthermore, a three-axis coordinate rotation was applied so that mean u, v, w, and the covariances between them equalled zero (Tanner & Thurtell, 1969). We calculated λE and F_c from the rotated covariances of w and S_{H_2O} and S_{CO_2}, respectively. An approximation of the half-hourly mean flux of F_s was calculated with:

$$F_s = h_m \overline{\rho_{air}} \frac{\Delta \overline{S}_{CO_2}}{\Delta t}, \tag{1}$$

where h_m is the height of the EC instrumentation (m), $\overline{\rho_{air}}$ is the mean molar density of dry air (mmol m^{-3}), and $\Delta \overline{S}_{CO_2}$ is the difference between the mean $\overline{S}_{CO_2}$ of the previous and the subsequent half-hours, respectively. Finally, the half-hourly NEE time series data (μmol m^{-2} s^{-1}) was calculated as the sum of F_c and F_s, and the half-hourly ET time series data (mm day^{-1}) was derived from λE. Neither NEE nor ET were corrected for the lack of surface energy balance closure. However, as an indicator for EC system performance, we evaluated energy closure for the snow-free periods by comparing the sum of the turbulent flux densities $H + \lambda E$ against independently measured available energy ($R_a = R_{net} - G$), integrated over periods when G summed to zero. The closure fractions were 0.82, 0.69, 0.79, and 0.82 for 2003–2006, respectively, and are comparable to those reported for other sites (Wilson *et al.*, 2002).

Gaps due to missing data are a common characteristic of high frequency EC time series data. Additional data gaps are introduced through screening the half-hourly EC time series data for outliers and for stable atmospheric conditions with low turbulent mixing. It was estimated that the annual coverage of EC time series data is reduced to approximately 65% on average due to missing and screened data (Falge *et al.*, 2001). At the SF site, 57% and 58% of all possible NEE and λE data points ($n = 35\,328$), respectively, were available after screening (Table 1).

Before screening the half-hourly NEE time series data, we first separated them into day- and night-time periods ($PAR_{in} < 4$ μmol m^{-2} s^{-1}). For outlier detection, we applied the technique described by Papale *et al.* (2006) to day- and night-time periods [with a 'conservative' z-value of 5.5 for Eqns (2) and (3) in Papale *et al.*, 2006]. We investigated the issue of the influence of stable atmospheric conditions on NEE measurements during night-time periods using the common approach of a 'friction velocity (u_*) – threshold'. A scatterplot of u_* vs. night-time NEE data points from all four snow-free periods (data not shown) showed small variation in NEE at higher values of u_*. However, at lower values of u_* ($u_* < 0.055$ m s^{-1}), NEE varied over a wide range from around −16 μmol m^{-2} s^{-1} (unrealistically indicating massive night-time CO_2-uptake), up to around 30 μmol m^{-2} s^{-1}. This overall pattern is in accordance with what was reported for other northern peatland sites (e.g., Lafleur *et al.*, 2001; Arneth *et al.*, 2002), but contrasts the general decrease in night-time NEE with decreasing u_* that was shown to result in night-time NEE underestimation. Despite the subjectivity of defining a u_*-threshold based on visual inspection (Gu *et al.*, 2005), night-time NEE data points with $u_* < 0.055$ m s^{-1} were discarded. Similar to NEE, the half-hourly λE time series data was first separated into day- and night-time periods and subsequently screened for outliers after Papale *et al.* (2006) with a conservative z-value of 5.5. The half-hourly λE time series data were not screened for stable atmospheric conditions.

The calculation of daily and seasonal totals of NEE, R_{eco}, GEE, and ET from incomplete half-hourly NEE and λE time series data requires the application of a gap-filling/flux-partitioning technique. A recent study showed a modest impact of most techniques on calculated annual totals of NEE (Moffat *et al.*, 2007). This study also demonstrated the general applicability of simple non-linear least square regression-based gap-filling techniques as originally introduced by Falge *et al.* (2001). We filled smaller gaps (<3 h) in the NEE time series data with linear interpolation and larger gaps (≥ 3 h) with a technique that uses modelled R_{eco} and GEE driven by $T_{air\text{-}2\,m}$ and PAR_{in}, respectively, to complete the half-hourly NEE time series data (Desai *et al.*, 2005). To estimate the uncertainty in total NEE,

Table 1 Percentages of missing NEE (μmol m^{-2} s^{-1}) and λE (W m^{-2}) half-hourly data points (n) for the snow-free periods of 2003–2006 (max. $n = 8832$)

Parameter	Flux	2003	2004	2005	2006
Missing n (of which are night-time)	NEE	44 (60)	47 (60)	27 (60)	29 (60)
Missing n* after screening (of which are night-time)	NEE	50 (86)	54 (87)	33 (78)	35 (80)
Missing n after short-term (<3 h) gap-filling† (of which are night-time)	NEE	43 (82)	47 (82)	24 (72)	25 (73)
Missing n (of which are night-time)	λE	44 (60)	47 (60)	25 (60)	25 (60)
Missing n* after screening (of which are night-time)	λE	50 (86)	54 (86)	31 (77)	32 (78)
Missing n after short-term (<3 h) gap-filling† (of which are night-time)	λE	43 (82)	47 (82)	22 (70)	22 (71)

*Outlier detection after Papale *et al.* (2006) and u_*-threshold ($u_* < 0.055$ m s^{-1}).
†Gap-filled with linear interpolation.

R_{eco}, and GEE due to gap-filling/flux-partitioning, we created 999 artificial incomplete half-hourly NEE time series data sets by bootstrapping the original incomplete half-hourly NEE time series data (Efron & Tibshirani, 1993). Each data point (including data gaps) of the original data set is sampled with the same probability and can occur multiple times in each artificial data set or not at all. In addition, each data point of the artificial data sets was randomly increased or decreased by 20% to account for the uncertainty inherent in the EC measurements themselves (Wesely & Hart, 1985). These artificial data sets were gap-filled and partitioned into their component fluxes after Desai *et al*. (2005), and summed. The uncertainty in each total of NEE, GEE, R_{eco} is reported as the SD of the respective mean total obtained from the original time series data sets plus 999 bootstrapped artificial time series data sets. We use the atmospheric sign convention so that negative NEE indicates net CO_2 uptake by the ecosystem whereas a positive NEE indicates net CO_2 loss to the atmosphere.

Similar to NEE, we filled smaller gaps (<3 h) in the half-hourly λE time series data with linear interpolation. Larger gaps ($\geq$ 3 h) were filled with the mean diurnal variation approach of Falge *et al*. (2001). The uncertainty in the totals of ET due to gap-filling was estimated as for NEE.

Hydrological measurements

The hydrological data set consisted of hydraulic head (h; m a.s.l.), WT (m a.s.l.), and ground surface (m a.s.l.) elevation measurements from a piezometer located about 150 m from the tower. We assume that this piezometer location is representative for the hydrological conditions within the footprint of the tower. Technical details on the installation of the piezometer and the measurement procedures are outlined in Hogan (2005) and Hogan *et al*. (2006). In brief, continuous hydraulic head measurements within the glaciofluvial sand underneath the SF site were made with a levelogger (model Solinst 3001 M5, Solinst Ltd., Georgetown, ON, Canada) every 30 min. Manual WT elevation was measured at 1-week to 1-month intervals using an electronic water-level tape (model Solinst 101 and 101 Mini, Solinst Ltd.). Manual ground surface elevation measurements were made at 1-week to 1-month intervals using a bog shoe (Roulet *et al*., 1991). Repeated manual ground surface elevation measurements during 2003 and 2004 made along a 100 m transect extending north of the piezometer showed that the entire ground surface moves in unison, with no significant differences between ridges and swales (Hogan, 2005). Continuous ground surface elevation measurements were made at a nearby location by means of a sonic sensor (model SR50; Campbell Scientific) mounted above a black-painted target platform attached to a bog shoe starting in October 2003. The signal was logged by a datalogger (model CR10X, Campbell Scientific) using a scan period of 1 min and recorded as half-hourly mean values. We compiled a mean daily ground surface elevation time series based on the continuous measurements. For the time before October 2003, we used the manual measurements with the missing days filled by linear interpolation. Daily WTD was calculated as the difference between mean daily ground surface elevation and mean daily *h* (i.e., positive WTD: WT below the ground surface; negative WTD: WT above the ground surface). The ground surface elevation at the continuous measurement location is equal to the average ground surface elevation of the nearby swales (Hogan, 2005). A WTD of 0 therefore corresponds to the water level being within a few centimeters above or below the ground surface in the swales and up to 0.30 m below ground surface beneath the ridges.

Analyses

In addition to daily and seasonal totals of NEE, R_{eco}, GEE, and ET, we performed different analyses. Correlation (Pearson's product-moment correlation coefficient) and regression analyses between daily R_{net} and WTD and ET, respectively, and between T_{soil} and WTD and GEE and R_{eco}, respectively, were performed for days with more than 36 half-hourly data points after filling of short gaps (Table 1).

Initial diagnostics using ordinary least-square (OLS) regression indicated heteroscedascity and the presence of influential outliers. To overcome the violation of OLS regression assumptions, we employed robust multiple regression (iterated re-weighted least-square fitting) with a re-descending M-estimator (Tukey) to quantify the relative influence of R_{net} and WTD on log-transformed daily ET:

$$\ln(\mathrm{ET}) = a + bR_{\mathrm{net}} + cWTD^2 + \varepsilon, \tag{2}$$

where a, b, and c are regression coefficients, and ε is the residual. Similarly, we used robust multiple regression to quantify the relative influence of T_{soil} and WTD on log-transformed daily GEE and R_{eco}

$$\ln(Y) = a + bT_{\mathrm{soil}} + cWTD + \varepsilon, \tag{3}$$

where Y is either GEE ($1\,\mathrm{g\,C\,m^{-2}\,day^{-1}}$ was added due to some slightly negative values) or R_{eco}, a, b and c are regression coefficients, and ε is the residual. We used the variance of inflation factor (VIF) as a measure for potential multicollinearity. The relative importance of the predictor variables (and the bootstrap confidence interval of their differences) in Eqns (3) and (4) was calculated after Lindeman *et al*. (1980, p. 119ff) as implemented by Groemping

(2006) in the relaimpo package for the R (v2.7.1) computing environment (R Development Core Team, 2008). The application of the relaimpo package to robust multiple regression followed Groemping (2007).

We calculated bulk surface conductance g_c (Monteith, 1965) and the Priestley–Taylor α_{PT} coefficient (Priestley & Taylor, 1972) as two ET-related bulk parameters from half-hourly mid-day (10:00–14:00 hours) gap-filled λE time series data. Daily and monthly mid-day means of g_c ($m\,s^{-1}$) for λE were calculated through inversion of a rearranged Penman–Monteith equation (e.g., Humphreys *et al*., 2006; Ryu *et al*., 2008). Owing to reasons outlined above (Data handling and processing of EC measurements), we were not able to calculate R_a as used in the Penman–Monteith equation directly from an independent set of measurements for the snow-free periods of 2004–2006. Instead, we approximated R_a as the sum of λE and H, thus avoiding the issue of energy-balance nonclosure.

The Priestley–Taylor α_{PT} coefficient is defined as the ratio of measured λE to equilibrium latent heat flux, $\lambda E_{Equlibrium}$, thereby indicating evaporation efficiency. Daily and monthly mid-day values for α_{PT} of approaching 1 are indicative for evaporation occurring at rates in the order of the potential rates, thus indicating unlimited water supply. We calculated α_{PT} from $\lambda E_{Equlibrium}$ using half-hourly data points at least 10 hours after the last rainfall:

$$\lambda E_{Equilibrium} = \frac{\Delta \times R_a}{(\Delta + \gamma)}, \quad (4)$$

where γ is the psychrometric constant. We used the following relationship comprising the hyperbolic GEE-PAR_{in} relationship of Michaelis & Menten (1913) and the exponential $R_{eco}-T_{air\_2\,m}$ relationship of the well-established Q_{10} model:

$$NEE = -\frac{\alpha \times PAR_{in} \times A_{max}}{\alpha \times PAR_{in} + A_{max}} + R_{10} \times Q_{10}^{(T_{air\_2\,m} - T_{10})/10} \quad (5)$$

to calculate α, the effective quantum yield ($\mu mol\,CO_2\,\mu mol\,PAR_{in}$), and A_{max}, the maximum photosynthetic capacity ($\mu mol\,m^{-2}\,s^{-1}$), as mid-summer (1 June–30 September) GEE-related bulk parameters, and R_{10}, i.e. the R_{eco} at 10 °C ($\mu mol\,m^{-2}\,s^{-1}$), and Q_{10}, i.e. the relative R_{eco} increase for a temperature increase of 10 °C as mid-summer R_{eco}-related bulk parameters from half-hour values of NEE, PAR_{in}, and $T_{air\text{-}2\,m}$ time series data. All four variable parameters, i.e. α, A_{max}, R_{10}, and Q_{10} (and their confidence intervals) were determined through unconstrained, nonlinear least-square regression (Levenberg–Marquardt algorithm). Calculation of the ET-, GEE-, and R_{eco}-related bulk parameters was performed using the MATLAB (v7.5) computing environment (The MathWorks Inc., 2007, Matlab, v7.5, The MathWork, Matick, MA, USA).

Results

Meteorological and resulting hydrological conditions

The meteorological conditions varied substantially among the snow-free periods of 2003–2006: 2003 was warm and dry, 2004 was cool and wet, and 2005 and 2006 were both wet (Fig. 1a). In 2003, total P was distributed fairly evenly, with about 67% occurring throughout June to September (normal: 82%) in the form of daily P events with usually <10 mm. This

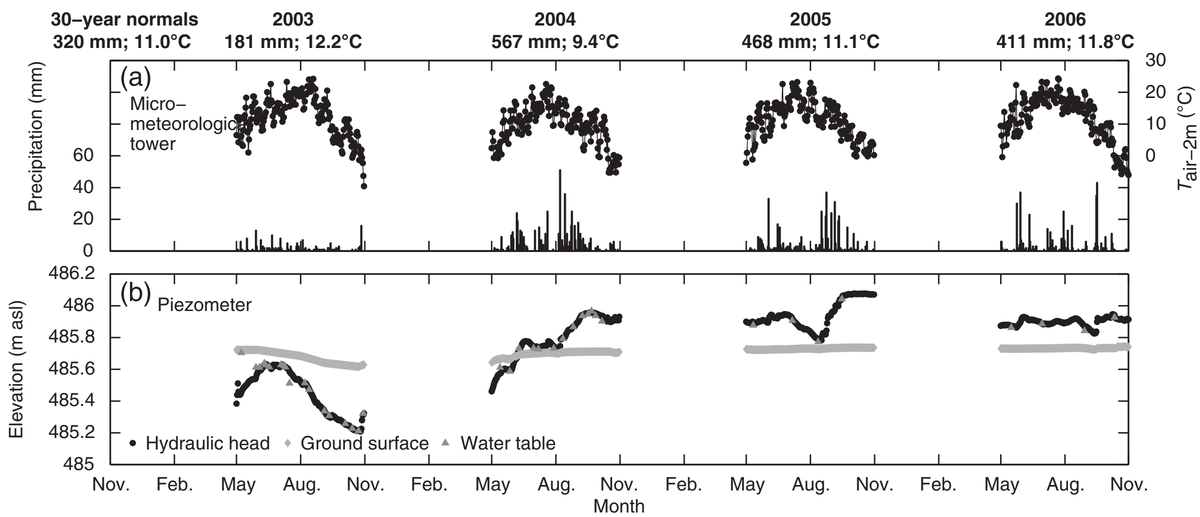

Fig. 1 Variations of (a) daily mean air temperature ($T_{air\text{-}2\,m}$; shown as lines) and total precipitation (P; shown as bars) and comparison of snow-free period means ($T_{air\text{-}2\,m}$) and totals (P), respectively, to 30-year normals, (b) daily mean hydraulic head (h), water table (WT), and ground surface elevations at the piezometer.

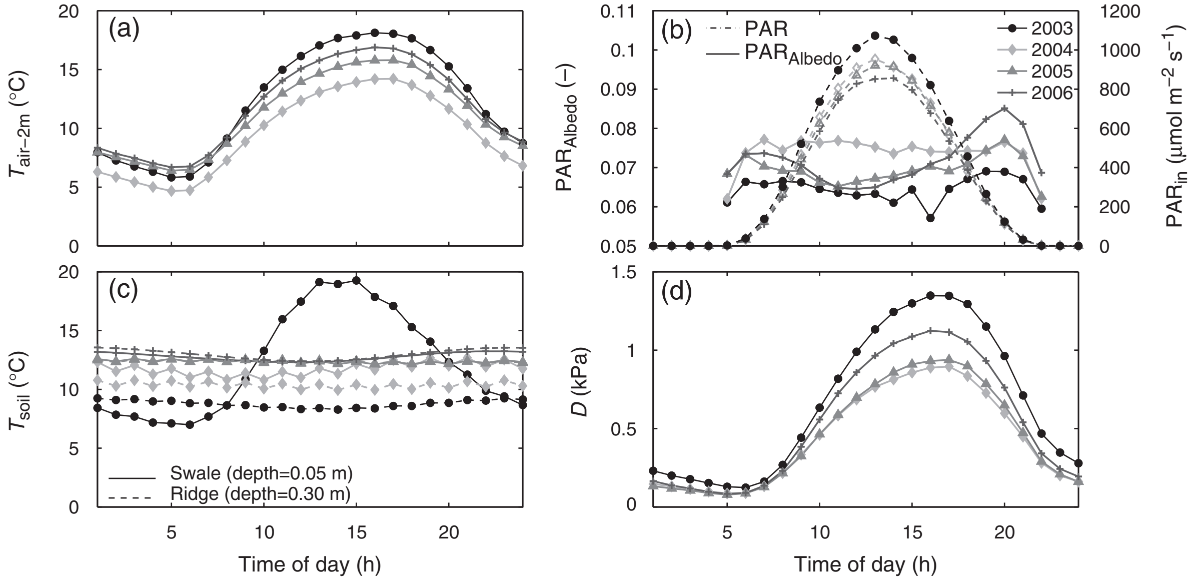

Fig. 2 (a) Mean diurnal patterns of air temperature ($T_{air\text{-}2\,m}$), (b) soil temperature (T_{soil}), (c) incoming photosynthetically active radiation (PAR_{in}) and PAR albedo (PAR_{Albedo}), and (d) vapor pressure deficit (D).

pattern changed substantially in 2004 when heavy P events started in early August. About 87% of the total P in the snow-free period of 2004 fell during June–September, 60% of which fell in August and September (normal: 40%), mostly in the form of daily P events with >10 mm. The two subsequent years were characterized by temporal patterns in daily P similar to 2004, i.e. summers that had about 83% and 73% of the total P with 64 (2005) and 53% (2006) in August and September. In all four snow-free periods, the SF site received similar amounts of K_{in} ($\sim 2.76\,GJ\,m^{-2}$). R_{net} was about 50% of K_{in} except for 2004 with 56%.

The switch from dry to wet conditions in 2004 was reflected in h, WT, and ground surface elevation (Fig. 1b). However, WTD was also strongly controlled by cold season processes related to the presence of a seasonal snow pack, which, through its influence on the vertical profile of T_{soil}, controls frost penetration depth (data not shown). After snowmelt in mid-April 2003, the presence of frozen peat until the end of May led to the formation of a perched WT, i.e. the localized occurrence of saturated conditions above the h that decoupled h and WT (Fig. 1b; WT$>$h). After the complete thawing of seasonally frozen peat and the disappearance of the perched WT by the end of May, WT $\sim$ h, both of which reached a minimum depth of around 0.05 m below the ground surface. As a result of dry conditions, both WT and h dropped to a maximum depth of about 0.4 m below the ground surface. In response to the pronounced changes in h and thus WT, the ground surface elevation dropped by around 0.20 m. In 2004, WT and h were similar to 2003 but due to higher P, the WT stayed slightly below or above the ground surface until the switch from dry to wet conditions. As a result of the continuing heavy P events, both WT and h continued to rise to a minimum ponding depth of -0.4 m above the ground surface (Fig. 1b). Owing to the more saturated and thus warmer peat profile at the end of the snow-free period, frost penetration in the following winter (2004–2005) was less deep (data not shown). After the rapid and complete thawing of the peat profile in 2005 (almost fully saturated) and 2006 (fully saturated), continued P caused the WT to stay well above the ground surface throughout each snow-free period. Under the resulting saturated peat profile in the wet years 2004–2006, ground surface elevation changes were negligible (<0.05 m).

The mean diurnal pattern in 5-cm T_{soil} in a swale during the dry conditions of 2003 followed the course of the mean diurnal pattern of $T_{air\text{-}2\,m}$ (Fig. 2a and b). However, based on a relief of about 0.25 m, the mean diurnal pattern in 30-cm T_{soil} on an adjacent ridge at the same absolute measurement elevation was completely dampened due to the greater relative measurement depth. During the wet snow-free periods (2004–2006), the topographic effects on the soil thermal regime diminished due to inundation, which completely damped mean diurnal patterns in $T_{soil\text{-}ridge\text{-}0.30\,m}$ and $T_{soil\text{-}swale\text{-}0.05\,m}$. Mean diurnal patterns in $T_{air\text{-}2\,m}$ (Fig. 2a), PAR_{in} (Fig. 2c), and D (Fig. 2d) reached the highest mid-day peaks in 2003, indicating generally less cloudy sky conditions and higher sensible heat fluxes, which is in accordance with 2003 being drier and warmer compared with the three subsequent years.

Table 2 Total evapotranspiration (ET), net ecosystem CO_2 exchange (NEE), gross ecosystem exchange (GEE), and total ecosystem respiration (R_{eco}) based on measured, filtered, and gap-filled/flux-partitioned time series data sets (Table 1) and mean total ET, NEE, GEE, and R_{eco} reported as the mean of 1000 ET, NEE, GEE, and R_{eco} totals calculated from the measured, filtered, and gap-filled time series data sets plus 999 bootstrapped artificial λE and NEE time series data sets (see text for more details)

Parameter Unit	ET (SD) mm period^{-1}	NEE (SD) g C m^{-2} period^{-1}	GEE (SD) g C m^{-2} period^{-1}	R_{eco} (SD) g C m^{-2} period^{-1}
2003	300; 315 (6)a	−2; 8 (7)a	317; 327 (15)a	315; 332 (15)a
2004	305; 315 (6)a	−170; −139 (11)b	508; 513 (32)b	338; 380 (34)b
2005	319; 316 (6)a	−157; −163 (8)c	414; 411 (14)c	256; 265 (13)c
2006	323; 316 (6)a	−190; −195 (9)d	448; 556 (23)d	297; 371 (24)d

The uncertainty in mean totals due to gap-filling (ET) and gap-filling/flux-partitioning (NEE, GEE, and R_{eco}), respectively, is reported as 1 SD. Different lowercase letters indicate that the totals are significantly different at $\alpha = 0.05$ (Tukey–Kramer's honestly significant difference criterion).

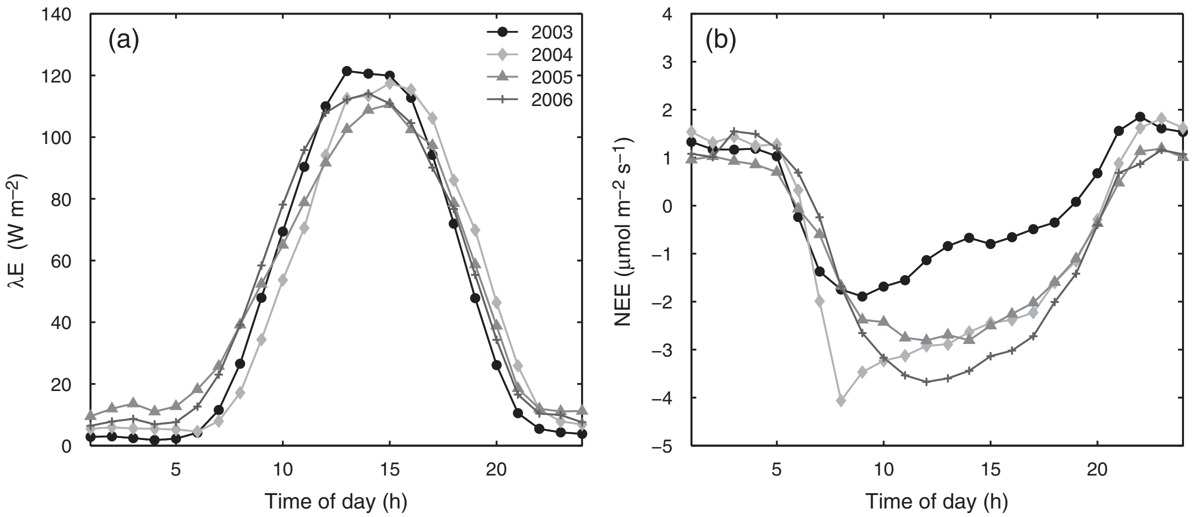

Fig. 3 Mean diurnal patterns of gap-filled (a) latent heat (λE) and (b) net ecosystem exchange (NEE).

The inundation in 2004–2006 also had a clear effect on the mean PAR albedo (PAR_{Albedo}) (Fig. 2c). PAR_{Albedo} is to a large extent controlled by the structure and especially the greenness of vegetation. In 2003, PAR_{Albedo} was generally lower than during the three subsequent wet years, the result of the lower vegetation abundance resulting in increased exposure of relatively 'dark' peat background. Furthermore, under wet conditions a certain fraction of the green vegetation was inundated (Fig. 1b). The surface of the ponded water is characterized by an oily film due to iron carbonate produced by the oxidation of ferrous iron in the presence of carbonate and bicarbonate in the pore water. This oily film may have caused parts of the SF site to appear 'brighter' and thus more reflective.

Evapotranspiration

Total ET varied only slightly among the four snow-free periods (Table 2). Taking into account the uncertainty due to gap-filling, the mean total ET of the 1000 time series data sets were not significantly different for $\alpha = 0.05$ (Table 2).

The mean diurnal pattern of λE was quite similar in all four snow-free periods. λE generally peaked between around noon and late afternoon (Fig. 3a). The peaks of λE roughly corresponded to the peaks of PAR_{in} occurring in the early afternoon (Fig. 2c) rather than to the peaks of D occurring later in the afternoon (Fig. 2d). Accordingly, daily ET was also quite similar between the four snow-free periods with a mean value (SD) of 1.69 (0.37) mm day^{-1} (Table 3; Fig. 4a).

Daily ET followed the seasonal variation of daily R_{net} (Fig. 4b). The high daily ET at the beginning of each snow-free period corresponded to increased daily R_{net} following snowmelt, when a perched WT stayed at or just below the ground surface (2003; 2004) or when the WT was well above the ground surface (2005; 2006). Daily ET was positively correlated with daily R_{net} (2003–2006: correlation coefficient (r) = 0.76, $P < 0.0001$,

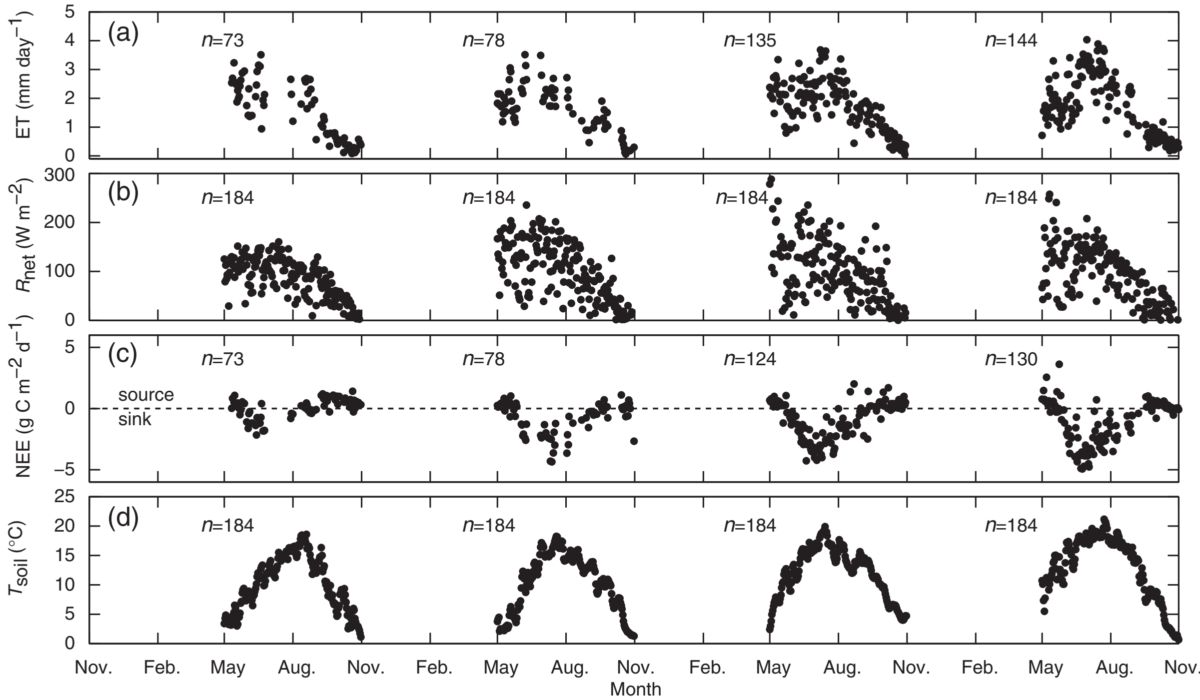

Fig. 4 (a) Daily evapotranspiration (ET) (mm day^{-1}), (b) daily net radiation (R_{net}) (W m^{-2}), (c) daily net ecosystem exchange (NEE) (g C m^{-2} day^{-1}), and (d) daily soil temperature (T_{soil}).

Table 3 Summary of mean daily (ET_{period}) and mean daily summer (ET_{summer}) ET, mean daily mid-day Priestley–Taylor coefficient (α_{PT}), and bulk surface conductance (g_c)

Parameter Unit	ET_{period} (SD) mm day^{-1}	ET_{summer} (SD) mm day^{-1}	α_{PT} (SD) –	g_c (SD) m s^{-1}
2003	1.63 (0.95)a	2.23 (0.58)a	0.79 (0.25)a	0.0039 (0.0018)a
2004	1.65 (0.85)a	2.16 (0.71)a	1.04 (0.25)b	0.0045 (0.0016)b
2005	1.74 (0.86)a	2.17 (0.67)a	0.99 (0.31)b	0.0046 (0.0015)b
2006	1.76 (0.99)a	2.43 (0.75)b	1.03 (0.32)b	0.0045 (0.0013)b

Different lowercase letters indicate significantly different mean values (Tukey–Kramer's honestly significant difference criterion).

$n = 430$). For comparison with mean daily ET from other Canadian peatlands as provided by Lafleur *et al.* (2005a), we also calculated mean daily summer ET for the three summer months June–August (Table 3).

Mean daily mid-day α_{PT} indicates that ET occurred at potential rates under wet conditions (2004–2006), but at significantly lower rates in the dry conditions of 2003 (Table 3). Generally, g_c was significantly lower in 2003 when atmospheric demand was highest compared with the subsequent 3 years, which were not significantly different (Table 3). No pattern emerged for the relationship between daily mid-day (data not shown) or monthly g_c and D (Fig. 5a) but a parabolic relationship between monthly g_c and WTD (Fig. 5b). Monthly means of daily mid-day α_{PT} increased with increasing g_c only in 2003, but were insensitive to changes in g_c in 2004–2006 (Fig. 5b).

Net ecosystem CO_2 exchange

The totals of NEE, GEE, and R_{eco} varied substantially among years. In 2003, the SF site was almost CO_2 neutral but acted as moderate sink in 2004–2006 (Table 2). Taking into account the uncertainty due to gapfilling/flux-partitioning, the differences in the mean totals of NEE, GEE, and R_{eco} based on the 1000 time series data sets were all significantly different at $\alpha = 0.05$ (Table 2).

As expected, the mean diurnal pattern of NEE differed substantially. Generally, there was higher photosynthetic uptake (negative NEE) in 2004–2006 compared with 2003 (Fig. 3b). Nighttime losses of CO_2 due to R_{eco} when NEE = R_{eco} were just slightly different, not showing a consistent pattern.

The substantial difference in the diurnal pattern of NEE was reflected in daily NEE (Fig. 4c). The totals of GEE and R_{eco} and the mean diurnal patterns of NEE suggest that the differences in daily NEE were mainly due to differences in daily GEE rather than in R_{eco}. For correlation analyses we used daily T_{soil} (Fig. 4d) calculated as the mean of $T_{soil\text{-}ridge\_0.30}$ and $T_{soil\text{-}swale\_0.05}$ instead of $T_{air\_2\,m}$, because the latter was used for gap-filling/flux-partitioning. Daily GEE and R_{eco}, were both positively correlated with daily mean T_{soil} (GEE 2003–2006: $r = 0.77$, $P < 0.0001$, $n = 405$; R_{eco} 2003–2006: $r = 0.78$, $P < 0.0001$, $n = 405$).

We assessed the response of half-hourly NEE to PAR and $T_{air\_2\,m}$ with Eqn (6) (Table 4). One of the two GEE-related bulk parameters, A_{max}, showed a continuous increase over the four snow-free periods. The other GEE-related bulk parameter, α, did not show a consistent pattern or trend. Similarly, the two R_{eco}-related bulk parameters, R_{10} and Q_{10}, did not reveal any clear pattern.

Influence of WTD on evapotranspiration and net ecosystem CO_2 exchange

Because of the broad range in WTD, spanning drought to flooding, the data were stratified into two WTD classes, above and below the flux optimum. Daily ET was weakly positively correlated with WTD when the WT was above (WTD ≤ 0) and negatively correlated with WTD when the WT was below the ground surface (WTD > 0) (Fig. 6a). The scatterplot of daily NEE vs. WTD suggests that maximum net CO_2 uptake occurred when the WT was slightly above the ground surface ($0 < \text{WTD} < -0.20$ m; Fig. 6b), declining for both higher and lower WTD. For example, in 2004 with the switch from dry to wet conditions, net CO_2 uptake increased as

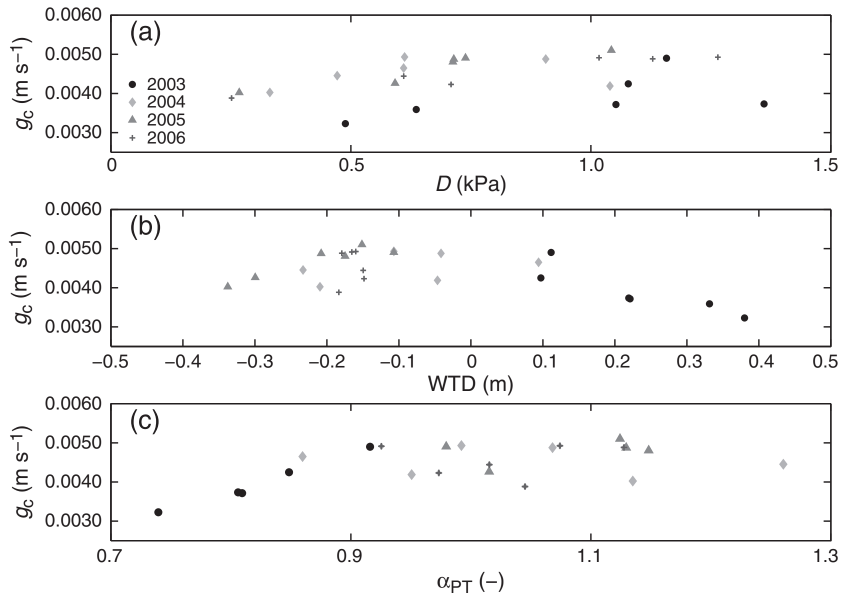

Fig. 5 Relationships between monthly means of daily mid-day bulk surface conductance (g_c) and (a) vapor pressure deficit (D), (b) water table depth (WTD), and (c) Priestley–Taylor coefficient (α_{PT}).

Table 4 Mid-summer (1 June–30 September) model parameters for Eqn (4) as determined through non-linear least-square regression (CI = 95% confidence interval)

Parameter Unit	α (CI) μmol CO_2 mol^{-1} PAR^{-1}	A_{max} (CI) μmol m^{-2} s^{-1}	R_{10} (CI) μmol m^{-2} s^{-1}	Q_{10} (CI) –
2003	0.076 (0.067; 0.085)	10.81 (10.42; 11.21)	3.32 (3.16; 3.48)	1.51 (1.46; 1.56)
2004	0.103 (0.092; 0.114)	16.30 (15.68; 16.91)	3.67 (3.44; 3.89)	1.06 (0.98; 1.14)
2005	0.043 (0.040; 0.046)	19.91 (19.04; 20.79)	2.57 (2.42; 2.73)	1.31 (1.23; 1.40)
2006	0.040 (0.038; 0.043)	28.17 (26.83; 29.50)	2.95 (2.79; 3.10)	1.18 (1.12; 1.25)

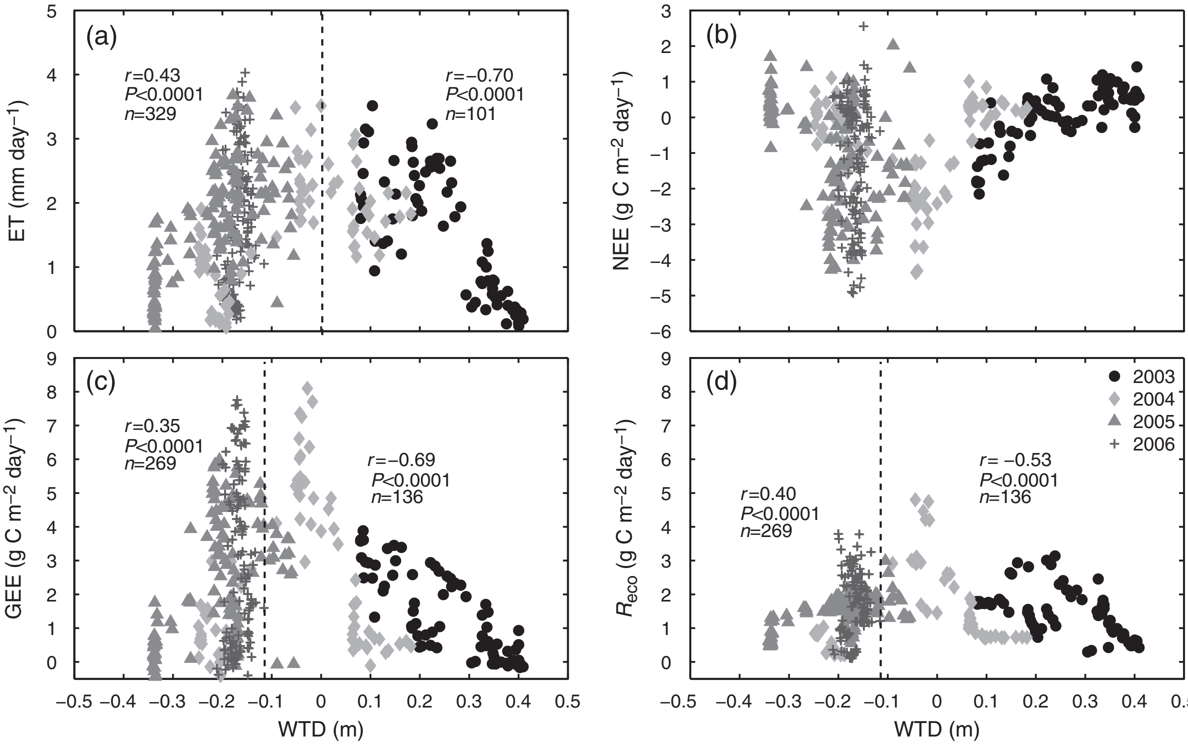

Fig. 6 Scatterplots of daily (a) evapotranspiration (ET), (b) net ecosystem exchange (NEE), (c) gross ecosystem productivity (GEE) and (d) total ecosystem respiration (R_{eco}) rates and water table depth (WTD). Stippled lines indicate WTD thresholds (ET: 0 m; GEE, R_{eco}: −0.11 m) as discussed in the text.

Table 5 Robust multiple regression coefficients (a, b, c) for daily evapotranspiration (ET) and net Radiation (X_1: R_{net}) and water table depth (X_2: WTD), and gross ecosystem exchange (GEE) and soil temperature (X_1: T_{soil}) and WTD (X_2), and ecosystem respiration (R_{eco}) and T_{soil} (X_1) and WTD (X_2) (type of regression (Reg. type): l = linear, q = quadratic; n = number of data points; Residual SE = residual standard error; R^2 = coefficient of multiple determination; X_1 = relative importance of X_1; X_2 = relative importance of X_2; CI = 95% confidence interval)

	WTD (m)	Type	n	a	b	c	Residual SE	R^2	X_1 (−)	X_2 (−)	X_1−X_2 (CI) (−)
ln(ET) ~ R_{net} + WTD	–	l + q	430	−0.11	0.01	6.24	0.46 (mm day^{-1})	0.68	0.67	0.33	0.34 (0.21; 0.49)
ln(GEE) ~ T_{soil} + WTD	> −0.11	l + l	136	1.07	0.04	−1.47	0.19 (g C m^{-2} day^{-1})	0.81	0.53	0.47	0.06 (−0.07; 0.21)
ln(GEE) ~ T_{soil} + WTD	≤ −0.11	l + l	269	0.66	0.08	8.05	0.27 (g C m^{-2} day^{-1})	0.74	0.89	0.11	0.78 (0.69; 0.86)
ln(R_{eco}) ~ T_{soil} + WTD	> −0.11	l + l	136	0.98	0.04	−0.37	0.08 (g C m^{-2} day^{-1})	0.86	0.78	0.22	0.56 (0.40; 0.71)
ln(R_{eco}) ~ T_{soil} + WTD	≤ −0.11	l + l	269	0.85	0.04	0.41	0.10 (g C m^{-2} day^{-1})	0.82	0.90	0.10	0.79 (0.70; 0.87)

the WT rose to an optimum negative WTD above the ground surface, then declined as the WT rose further. Similar to NEE, both GEE and R_{eco} reached a maximum at a WTD of −0.11 m (WTD resulting in the lowest correlation coefficient for WTD vs. GEE and WTD vs. R_{eco} for WTD > −0.11 m). Daily GEE and R_{eco} were both negatively correlated with WTD for WTD > −0.11 m and more weakly positively correlated with WTD for WTD ≤ −0.11 m (Fig. 6c and d).

We evaluated the relative importance of WTD for the daily variation of water vapor and CO_2 fluxes compared with other important environmental controls (Evapotranspiration, Net ecosystem CO_2 exchange), R_{net} (ET) and T_{soil} (GEE; R_{eco}), through robust multiple regression. The quadratic term in Eqn (3) accounts for an optimal response of ET to WTD. R_{net} and WTD account for 68% of the variation in daily ET. The contributions of R_{net} and WTD were 67% and 33%, which suggests that ET generally follows the seasonality of R_{net} and is only weakly controlled by WTD (Table 5). As indicated by VIF = 1.37, very weak multicollinearity between R_{net} and WTD may be present.

For GEE and R_{eco}, the regressions were run twice, for WTD above and below the WTD optimum of -0.11 m. Under drier conditions (WTD > -0.11 m), T_{soil} and WTD together account for 81% of the explained variation in daily GEE. Daily WTD contributes almost half to the explained variation and there is no significant difference between the contributions of WTD and T_{soil} (Table 5). For wetter conditions (WTD ≤ -0.11 m) in contrast, the contribution of WTD to the explained variation in daily GEE is minor (Table 5). For both WTD > -0.11 m and WTD ≤ -0.11 m, only very weak multicollinearity was found (VIF = 1.35 for both WTD > -0.11 m and WTD ≤ -0.11 m). R_{eco} responded differently. Daily R_{eco} is strongly related to T_{soil} for both dry (WTD > -0.11 m) and wet (WTD ≤ -0.11 m) conditions, which suggests that R_{eco} generally follows the seasonality of T_{soil} and WTD is a minor influence (Table 5). Again, for both WTD > -0.11 m and WTD ≤ -0.11 m, only very weak multicollinearity may exist (WTD > -0.11 m: VIF = 1.28; WTD ≤ -0.11 m: VIF = 1.36).

Discussion

Evapotranspiration

As indicated by mean daily summer rates (Table 3), ET at the SF site fell into the range of values reported for various peatlands in Canada (Lafleur *et al.*, 2005a; Humphreys *et al.*, 2006). The difficulty in understanding peatland ET lies in the interaction of various factors including fluctuations of a shallow WT above or below the ground surface, resulting in increased complexity compared with other ecosystems. As a result, relationships that hold for upland ecosystems, such as g_c vs. D, may be weak or insignificant for peatlands (e.g., Humphreys *et al.*, 2006; Pejam *et al.*, 2006; Ryu *et al.*, 2008). At the SF site, substantial fluctuations in WTD created extreme hydrological and ecological conditions that are characteristic for interior, central Canada.

The role of WTD on peatland ET is still uncertain (Lafleur *et al.*, 2005a). For example, Kim & Verma (1996) and Kellner (2001) found for a fen in Minnesota and a bog in Sweden, respectively, that WTD exerted some control over ET. In contrast, the data presented by Lafleur *et al.* (2005a) for a bog in Canada suggests that WTD had almost negligible influence on ET. An intercomparison study of seven peatlands across Canada (including the SF site) for July and August 2004 does not show any notable influence of WTD on ET (Humphreys *et al.*, 2006).

A recent conceptual peatland ET model by Lafleur *et al.* (2005a) suggests bogs and poor fens show a limited response of ET to WTD fluctuations up to a critical depth (0.65 m at the Mer bleue bog in Ontario, Canada) when root water-uptake of vascular plants might stop and water extraction of *Sphagnum* mosses in hollows through capillary forces becomes limited. The presence of *Sphagnum* mosses guarantees wet ground surface conditions over a wide range of WTD, dampening the response of g_c to D due to reduced ground surface resistance ($g_{ground}^{-1} = f_{soil} \times g_{soil}^{-1} + f_{mosses} \times g_{mosses}^{-1} + f_{water} \times g_{water}^{-1}$ with f_{soil}, f_{mosses}, and f_{water} being the relative hypothetical fractions of soil, mosses, and open water, respectively). Theoretically g_{ground}^{-1} approaches zero with the start of water ponding ($= 0 \times g_{soil}^{-1} + 0 \times g_{mosses}^{-1} + 1 \times g_{water}^{-1}$ and $g_{water}^{-1} = 0$). Under these conditions, variations in g_c are a function of vascular plants and thus stomatal conductance ($g_{stomata}$) only. In contrast to *Sphagnum* mosses, brown mosses are not able to remain as wet through capillary forces as *Sphagnum* mosses do (Janssens *et al.*, 1992) and thus are more sensitive to WTD fluctuations. At the SF site, WTD under dry conditions was never as high as at the Mer Bleue bog under dry conditions (~ 0.75 m). Owing to the differences in vascular plant and moss species, a maximum WTD of just 0.4 m was probably sufficient to cause vegetation stress due to drought. It does not seem surprising to see an influence of WTD on ET, which is similar in terms of maximum WTD to the peatland sites of Kellner (2001) and Kim & Verma (1996).

The conceptual model of Lafleur *et al.* (2005a) was complemented through analysis of the different responses of g_c to D obtained from various peatland sites (Humphreys *et al.*, 2006). In Humphreys *et al.* (2006) and Fig. 5a, the SF site showed only a very weak and no response, respectively, of g_c to changes in D. Our data show no clear relationship between g_c and D under the wet conditions of 2004–2006 due to ponding water. No clear response of g_c to changes in D under dry conditions was found, but instead a parabolic relationship between g_c and WTD combined for dry and wet conditions combined (Fig. 5b). The parabolic response of g_c to changes WTD suggests that daily ET is comprised of varying contributions from different ground surface components (bare soil, mosses, and ponding water) and vascular plants in response to the seasonal variation in R_{net} as regulated by WTD.

In 2003, WTD increased continuously after snowmelt. As a result, g_c decreased mainly due to increased g_{ground}^{-1} ($= f_{soil}(\Uparrow) \times g_{soil}^{-1} + f_{mosses}(\Uparrow) \times g_{mosses}^{-1} + 0 \times g_{water}^{-1}$ with $\Downarrow$ and $\Uparrow$ indicating decrease and increase, respectively, of the respective hypothetical fraction), and to some degree due to increased g_{canopy}^{-1} (i.e., $g_{stomata}^{-1}$ at ecosystem scale, which is a function of vascular plant abundance expressed through aboveground biomass or LAI) in response to increasing D, resulting in lower rates of daily ET.

After the switch from dry to wet conditions in 2004, the WT stayed at the ground surface similar to 2003, but

WTD started to continuously decrease with increased P. A continuously larger proportion of the ground surface and vascular plants was covered by ponding water. As a result, g_c decreased (Fig. 5) because of the decrease in vascular plant abundance since g_c was continuously more controlled by g_{canopy}^{-1} alone due to the continuous decrease of $g_{surface}^{-1}$ ($= f_{soil}$ ($\Downarrow$) $\times g_{soil}^{-1} + f_{mosses}$ ($\Downarrow$) $\times g_{mosses}^{-1} + f_{water}(\Uparrow) \times g_{water}^{-1}$). Because *Carex* spp. are well-adapted to wet conditions (e.g., Bubier *et al*., 2003), the reported effect of partial stomatal closure under saturated conditions (Zhang & Davies, 1987; Else *et al*., 1996) was rather negligible and aboveground biomass or LAI was most likely higher in 2004–2006 (LAI_{wet}) than in 2003 (LAI_{dry}). If $LAI_{wet} \gg LAI_{dry}$, then a reduction in LAI_{wet} due to inundation should still result in higher values for g_{canopy} under wet compared with dry conditions and explain the reduced sensitivity of g_c under wet conditions. Unfortunately, no aboveground biomass or LAI data exists to investigate this hypothesis.

In 2005, the WT fluctuated above the ground surface and varying proportions of vascular plants were inundated. A notable increase in WTD at mid-August caused the WT to almost reach the ground surface when R_{net} was about highest. As a result, g_c, as mainly controlled by g_{canopy}^{-1} increased because a smaller proportion of vascular plants was covered by ponding water, resulting in the highest rates of daily ET. The increase in WTD did not affect the relative hypothetical fractions of soil, mosses, and open water since the SF site was still inundated, i.e. $g_{surface}^{-1} = 0 \times g_{soil}^{-1} + 0 \times g_{mosses}^{-1} + 1 \times g_{water}^{-1}$ and $g_{water}^{-1} = 0$. The mid-August increase in WTD was followed by a WTD decrease, i.e. an increasing proportion of vascular plants covered with ponding water.

In 2006, the WT was stagnant and stayed above the ground surface. Consequently, the proportion of vascular plants covered by ponding water under saturated conditions was constant and not controlled by WTD fluctuations resulting in changes in g_c through changes in $g_{surface}^{-1}$ ($= 0 \times g_{soil}^{-1} + 0 \times g_{mosses}^{-1} + 1 \times g_{water}^{-1}$). As a result, daily ET rates were a function of the seasonal cycle of R_{net} alone.

Overall the contributions of vascular plants and different ground surface components under varying meteorological conditions appear to compensate each other. For example, the reduced contribution from bare soil, mosses, and vascular plants to total ET is compensated by the contribution from open water, as indicated by the insignificant differences in total ET (Table 2).

Net ecosystem CO_2 exchange

The importance of WTD for peatlands' C balance has been emphasized in various studies from different perspectives (e.g., Bubier *et al*., 2003; Lindroth *et al*., 2007; Yurova *et al*. 2007). Our analyses show that NEE from the SF site responded differently to dry and wet conditions, which had no overall effect on total ET but most likely affected the contributions of vascular plants and different ground surface components. In contrast to ET where WTD has direct (e.g., the contribution of ponding water evaporation to ET) and indirect (e.g., earlier senescence due to drought) effects, a different picture emerges for GEE and R_{eco} which are controlled by WTD only indirectly. Decreased wetness caused vegetation stress and thus decreased g_c. The dry conditions in 2003 most likely resulted in earlier senescence (i.e. shorter growing season) of the generally less healthy and productive vascular plants that are well-adapted to wet conditions. Despite cooler temperatures in 2004, vascular plants were generally healthier and more abundant and productive due to increased wetness, resulting in higher GEE. In 2005 and 2006, both similarly wet but warmer than 2004, photosynthetic uptake remained high or even increased further. This further increase was most likely related to longer growing seasons due to the earlier thawing of the less deeply frozen peat profile. The effect of increased wetness on growing season length, especially onset and dormancy, was reported to be crucial for differences in NEE and especially GEE (e.g., Griffis *et al*., 2000; Sagerfors *et al*., 2008). A similar response of GEE to changes in meteorological conditions was reported for various other fen sites with similar species composition and nutrient status (e.g., Griffis *et al*., 2000; Bubier *et al*., 2003). Regarding R_{eco}, our results show that T_{soil} was a more dominant control than wetness, which is in accordance with several studies from a range of different peatland types (e.g., Bubier *et al*., 1998; Lafleur *et al*., 2005b; Lindroth *et al*., 2007). Overall, the variability in NEE was mainly controlled by the variability of GEE, which is supported by increased maximum photosynthetic capacity under wetter conditions with higher vegetation abundance. Humphreys *et al*. (2006) reported strong relationships between A_{max} and aboveground biomass and LAI, with higher A_{max} for sites with more aboveground biomass and higher LAI. Overall, the GEE- and R_{eco}-related bulk parameters α, A_{max}, R_{10}, and Q_{10} are approximately within the range of values provided by Frolking *et al*. (1998) and Humphreys *et al*. (2006) both of which include the SF site. The increased maximum photosynthetic capacity (A_{max}) under wetter conditions at the SF site is consistent with generally lower NEE due to higher GEE and is most likely related to increased vascular plants abundance.

Ultimately, water vapor and CO_2 fluxes are linked since photosynthesis, and transpiration and moss evaporation are tightly coupled through g_s and g_{moss}, respectively. The linkage of these two fluxes can be quantified through water use efficiency (WUE), which is the ratio of CO_2 uptake through photosynthesis and water vapor lost by the ecosystem through transpiration (vascular plants) or evaporation (mosses). WUE is commonly determined at the leaf-level and reported in units of mmol CO_2 mol H_2O^{-1} (Ponton *et al*., 2006). This 'real' leaf-level WUE was approximated through the ratio of EC-derived GEE and – measured ET at the ecosystem scale (e.g., Law *et al*., 2002; Humphreys *et al*., 2006). Understanding the temporal variability of ecosystems' WUE is crucial for the understanding of climate-change-induced alterations of the C and water cycles and thus ecosystem functioning. Our results show that such as an analysis would be misleading for ecosystems that experience both drought and inundation because of the varying contributions of different photosynthesizing (vascular plants, brown mosses) and nonphotosynthesizing (bare soil, open water) land surface sources to total ET. Understanding the water vapor contributions from different land surface sources has recently been identified as a responsibility of growing importance for the more realistic but more complex treatment of terrestrial water and C cycles in land surface schemes (Lawrence *et al*., 2007).

Conclusions

For this study we analyzed hydrological and micro meteorological measurements from four snow-free periods (2003–2006) from the Sandhill fen in central Saskatchawan, Canada. The goal was to explore the relationship between fluctuations in daily WTD and water vapor and CO_2 fluxes. The results of our study provide important insights into these complex relationships: WTD has a negligible effect on total ET, which appears to be due to the impact of WTD on g_c and thus the compensating contributions of vascular plants and different ground surface components. Furthermore, WTD is only of secondary importance for explaining variations in daily ET relative to radiation and thus seasonality. However, WTD has a considerable effect on daily NEE, mostly due to the influence of WTD on GEE. Up to a minimum ponding depth, about half (relative to temperature and thus seasonality) the explained variation in daily GEE is contributed by WTD. In contrast, the influence of WTD on daily R_{eco} appears to be of secondary importance regardless of WTD. The results of our study pose an important challenge to future modeling efforts focusing on peatlands similar to the SF site, namely, the (spatially) explicit consideration of subsurface and surface water flows in response to topography, hydrogeology, and meteorological conditions to allow for a more realistic simulation of peatland hydrology including ground surface elevation changes.

Acknowledgements

We thank Ankur Desai (University of Wisconsin-Madison) for sharing his gap-filling/flux-partitioning code. We also thank Matthias Peichl (McMaster University), Youngryel Ryu (University of California, Berkeley), Julie Talbot and Tim Moore (both McGill University) for their comments on earlier versions of this manuscript. Dell Bayne, Raoul Granger, Newell Hedstrom, and Randy Schmidt (all National Water Research Institute) are thanked for years of dedicated work at the SF site. We thank the Associate Editor and the two anonymous reviewers for their constructive comments that substantially improved the manuscript. This study was supported by Fluxnet-Canada Research Network and the Canadian Carbon Program funded by the Natural Science and Engineering Council of Canada, the Canadian Foundation of Climate and Atmospheric Sciences, and BIOCAP Canada, and the National Water Research Institute of Environment Canada.

References

Arneth A, Kurbatova J, Kolle O *et al*. (2002) Comparative ecosystem-atmosphere exchange of energy and mass in a European Russian and a central Siberian bog II. Interseasonal and interannual variability of CO_2 fluxes. *Tellus Series B-Chemical and Physical Meteorology*, **54**, 514–530.

Bhatti JS, Errington RC, Bauer IE, Hurdie FA (2006) Carbon stock trends along forested peatland margins in central Saskatchewan. *Canadian Journal of Soil Science*, **86**, 321–333.

Bubier JL, Bhatia G, Moore TR, Roulet NT, Lafleur PM (2003) Spatial and temporal variability in growing-season net ecosystem carbon dioxide exchange at a large peatland in Ontario, Canada. *Ecosystems*, **6**, 353–367.

Bubier JL, Crill PM, Moore TR, Savage K, Varner RK (1998) Seasonal patterns and controls on net ecosystem CO_2 exchange in a boreal peatland complex. *Global Biogeochemical Cycles*, **12**, 703–714.

Desai AR, Bolstad P, Cook BD, Davis KJ, Carey EV (2005) Comparing net ecosystem exchange of carbon dioxide between an old-growth and mature forest in the Upper Midwest, USA. *Agricultural and Forest Meteorology*, **128**, 33–55.

Efron B, Tibshirani RJ (1993) *An Introduction to the Bootstrap*. Chapman & Hall, New York.

Else MA, Tiekstra AE, Croker SJ, Croker SJ, Davies WJ, Jackson MB (1996) Stomatal closure in flooded tomato plants involves abscisic acid and achemically unidentified anti-transpirant in xylem sap. *Plant Physiology*, **112**, 239–247.

Falge E, Baldocchi DD, Olson R *et al*. (2001) Gap filling strategies for long term energy flux data sets. *Agricultural and Forest Meteorology*, **17**, 71–77.

Frolking S, Bubier JL, Moore TR *et al*. (1998) Relationship between ecosystem productivity and photosynthetically active radiation for northern peatlands. *Global Biogeochemical Cycles*, **12**, 115–126.

Gorham E (1991) Northern peatlands: role in the carbon-cycle and probable responses to climatic warming. *Ecological Applications*, **1**, 182–195.

Griffis TJ, Rouse WR, Waddington JM (2000) Interannual variability of net ecosystem CO_2 exchange at a subarctic fen. *Global Biogeochemical Cycles*, **14**, 1109–1121.

Groemping U (2006) Relative importance for linear regression in R: the package relaimpo. *Journal of Statistical Software*, **17**, 1–27.

Groemping U (2007) Re: [R] relative importance of predictors. Online posting, 29 November 2007. Available at http://tolstoy.newcastle.edu.au/R/ (Accessed 1 May, 2009).

Gu L, Falge E, Boden T *et al*. (2005) Objective threshold determination for nighttime eddy flux filtering. *Agricultural and Forest Meteorology*, **182**, 179–197.

Hogan JM (2005) *Hydrologic behavior and hydraulic properties of a patterned fen in Saskatchewan*. Unpublished MSc thesis, University of Saskatchewan, Saskatoon, Canada, 107 pp.

Hogan JM, van der Kamp G, Barbour SL, Barbour SL, Schmidt R (2006) Field methods for measuring hydraulic properties of peat deposits. *Hydrological Processes*, **20**, 3635–3649.

Humphreys ER, Lafleur PM, Flanagan LB, Flanagan LB, Hedstrom N, Syed KA, Glenn AJ, Granger R (2006) Summer carbon dioxide and water vapor fluxes across a range of northern peatlands. *Journal of Geophysical Research-Biogeosciences*, **111**, 1–16.

Janssens JA, Hansen DC, Glaser PH, Whitlock C (1992) Development of a raised bog complex. In: *The Patterned Peatland of Minnesota* (eds Wrigth HE, Coffin BA, Aaseng NE), pp. 189–221. University of Minneapolis-St. Paul, MN, USA.

Kellner E (2001) Surface energy fluxes and control of evapotranspiration from a Swedish Sphagnum mire. *Agricultural and Forest Meteorology*, **110**, 101–123.

Kim J, Verma SB (1996) Surface exchange of water vapour between an open *Sphagnum* fen and the atmosphere. *Boundary-Layer Meteorology*, **79**, 243–264.

Lafleur PM, Hember RA, Admiral SW, Roulet NT (2005a) Annual and seasonal variability in evapotranspiration and water table at a shrub-covered bog in southern Ontario, Canada. *Hydrological Processes*, **19**, 3533–3550.

Lafleur PM, Moore TR, Roulet NT, Frolking S (2005b) Ecosystem respiration in a cool temperate bog depends on peat temperature but not water table. *Ecosystems*, **8**, 619–629.

Lafleur PM, Roulet NT, Admiral SW (2001) Annual cycle of CO_2 exchange at a bog peatland. *Journal of Geophysical Research-Atmospheres*, **106**, 3071–3081.

Law BE, Falge E, Gu L *et al*. (2002) Environmental controls over CO_2 and water vapor exchange of terrestrial vegetation. *Agricultural and Forest Meteorology*, **113**, 97–120.

Lawrence DM, Thornton PE, Oleson KW *et al*. (2007) The partitioning of evapotranspiration into transpiration, soil evaporation, and canopy evaporation in a GCM: impacts on land-atmosphere interaction. *Journal of Hydrometeorology*, **8**, 862–880.

Lindeman RH, Merenda PF, Gold RZ (1980) *Introduction to Bivariate and Multivariate Analysis*. Scott, Foresman, Glenview, IL, USA.

Lindroth A, Lund M, Nilsson M *et al*. (2007) Environmental controls on the CO_2 exchange in north European mires. *Tellus*, **59B**, 812–825.

Maltby E, Immirzi P (1993) Carbon dynamics in peatlands and other wetland soils: regional and global perspectives. *Chemosphere*, **27**, 999–1023.

Michaelis L, Menten M (1913) Die Kinetik der Invertinwerkung. *Biochemische Zeitschrift*, **49**, 333–369.

Moffat AM, Papale D, Reichstein M *et al*. (2007) Comprehensive comparison of gap-filling techniques for eddy covariance net carbon fluxes. *Agricultural and Forest Meteorology*, **147**, 209–232.

Monteith JL (1965) Evaporation and the environment. In: *Proceedings of the 19th Symposium of the Society of Experimental Biology* (ed. Fogg GE), pp. 205–234. Cambridge University Press, Cambridge, UK.

Moore TR, Roulet NT, Waddington JM (1998) Uncertainty in predicting the effect of climatic change on the carbon cycling of Canadian peatlands. *Climatic Change*, **40**, 229–245.

Nilsson M, Sagerfors J, Buffam I *et al*. (2008) Contemporary carbon accumulation in a boreal oligotrophic minerogenic mire – a significant sink after accounting for all C-fluxes. *Global Change Biology*, **14**, 2317–2332.

Papale D, Reichstein M, Aubinet M *et al*. (2006) Towards a standardized processing of Net Ecosystem Exchange measured with eddy covariance technique: algorithms and uncertainty estimation. *Biogeosciences*, **3**, 571–583.

Pejam MR, Arain MA, McCaughey JH (2006) Energy and water vapour exchanges over a mixedwood boreal forest in Ontario, Canada. *Hydrological Processes*, **20**, 3709–3724.

Ponton S, Flanagan LB, Alstad KP *et al*. (2006) Comparison of ecosystem water-use efficiency among Douglas-fir forest aspen forest and grassland using eddy covariance and carbon isotope techniques. *Global Change Biology*, **2**, 294–310.

Priestley CHB, Taylor RJ (1972) On the assessment of surface heat flux and evaporation using large-scale parameters. *Monthly Weather Review*, **100**, 81–92.

R Development Core Team (2008) R: A language and environment for statistical computing. R Foundation for Statistical Computing, Vienna, Austria. ISBN 3-900051-07-0. Available at http://www.R-project.org (accessed 20 February 2009).

Roulet NT, Hardill S, Comer N (1991) Continuous measurements of the depth of water table (inundation) in wetlands with fluctuating surfaces. *Hydrological Processes*, **5**, 399–403.

Roulet NT, Lafleur PM, Richards PJH, Moore TR, Humphreys ER, Bubier J (2007) Contemporary carbon balance and late Holocene carbon accumulation in a northern peatland. *Global Change Biology*, **13**, 397–411.

Roulet NT, Munro DS, Mortsch L (1997) Wetlands. In: *The Surface Climates of Canada* (eds Bailey WG, Oke TR, Rouse WR), pp. 149–171. McGill-Queen's University Press, Montreal, QC, Canada.

Ryu Y, Baldocchi DD, Ma S, Hehn T (2008) Interannual variability of evapotranspiration and energy exchange over an annual grassland in California. *Journal of Geophysical Research-Atmospheres*, **113**, 1–16.

Sagerfors J, Lindroth A, Grelle A *et al*. (2008) Annual CO_2 exchange between a nutrient-poor minerotrophic, boreal mire and the atmosphere. *Journal of Geophysical Research-Biogeosciences*, **113**, 1–15.

Sellers PJ, Hall FG, Kelly RD *et al*. (1997) BOREAS in 1997: experiment overview scientific results, and future directions. *Journal of Geophysical Research-Atmospheres*, **102**, 28731–28769.

Suyker AE, Verma SB, Arkebauer TJ (1997) Season-long measurements of carbon dioxide exchange in a boreal fen. *Journal of Geophysical Research-Atmospheres*, **102**, 29021–29028.

Tanner CB, Thurtell GW (1969) Anemoclinometer measurements of Reynolds stress and heat transport in the atmospheric surface layer. US Army Electronics Comand Technical Report ECOM 66-G22-F, University of Wisconsin, Madison, WI, USA.

Turunen J, Tomppo K, Tolonen K *et al*. (2002) Estimating carbon accumulation rates of undrained mires in Finland: application to boreal and subartic regions. *Holocene*, **12**, 69–80.

Webb EK, Pearman GI, Leuning R (1980) Correction of flux measurements for density effects due to heat and water vapor transfer. *Quarterly Journal of the Royal Meteorological Society*, **106**, 85–100.

Wesely ML, Hart RL (1985) Variability of short term eddy correlation estimates of mass exchange. In: *The Forest-Atmosphere Interactions* (eds Hutchinson BA, Hicks BB), pp. 591–612. D. Reidel Publishing Co, Dordrecht, the Netherlands.

Wilson K, Goldstein A, Falge E *et al*. (2002) Energy balance closure at FLUXNET sites. *Agricultural and Forest Meteorology*, **113**, 223–243.

Yurova A, Wolf A, Sagerfors J, Nilsson M (2007) Variations in net ecosystem exchange of carbon dioxide in a boreal mire: modeling mechanisms linked to water table position. *Journal of Geophysical Research-Biogeosiences*, **112**, 1–13.

Zhang J, Davies WJ (1987) ABA in roots and leaves of ooded pea plants. *Journal of Experimental Botany*, **38**, 649–659.

Zoltai SC, Siltanen RM, Johnson JD (2000) A wetland database for the western boreal subarctic and arctic regions of Canada. Information Report NOR-X 368, Natural Resources Canada, Canadian Forest Service, Northern Forest Centre Edmonton, Alberta, Canada.